Part F: Harmonically-Forced Systems

Introduction - Resonance Effects

We have already seen many examples of how the presence of (compressive) axial load tends to reduce the lateral stiffness and hence natural frequencies. We shall now consider the effect of axial loads on the steady state response of forced structural systems. This section will focus on an important class of forcing functions, i.e., harmonic excitation. We typically then have a governing equation of motion of the form

$$M\ddot{x} + C\dot{x} + K(1-p)x = F_0 \sin \omega t, \tag{1}$$

in which M, K and C represent physical properties associated with a slender structural system. We again assume that the spring stiffness is reduced by the presence of a parameter p, later to be identified with axial load.

The solution of equation (1) consists of the summation of two parts. First, the homogeneous solution is obtained from the free vibration and was derived previously. For typical damping values it consists of an exponentially decaying oscillation (assuming $p < 1$). Second, the particular solution consists of a steady-state oscillation, $X_0 e^{i\omega t}$ where the magnitude of the steady-state response (relative to the forcing magnitude) is given by

$$\frac{X_0}{F_0} = R(\omega) = \frac{1}{\sqrt{(K(1-p) - \omega^2 M)^2 + (C\omega)^2}}, \tag{2}$$

and is often referred to as the receptance, amplitude response, or frequency response function (FRF). We observe the important resonant effect if the driving frequency ω is close to the natural frequency $\omega_n = \sqrt{K/M}$ of the system, or $\Omega = \omega/\omega_n = 1$.

The figure below shows the receptance for the parameter values $K = M = 1$ and $C = 0.2$, as a function of the destabilizing parameter p.

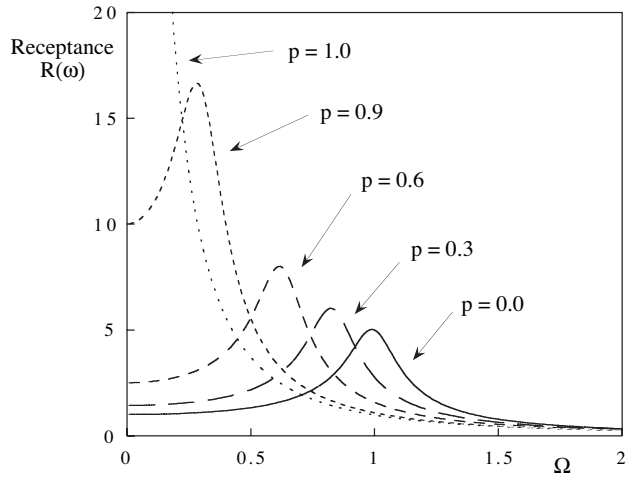

Effect of diminished stiffness on the receptance of a spring mass damper.

We note that increasing p tends to shift the resonant peaks toward lower frequencies (with negative p (tensile) having the opposite effect). The receptance could also have been nondimensionalized with respect to the effective stiffness in which case the curves would have emanated from a common point on the y-axis.

A Single-Mode Approximation

A single-mode energy analysis of a clamped-clamped beam-column, assuming a mode shape of the form

$$w(x,t) = \frac{Q(t)}{2}\left[1 - \cos\frac{2\pi x}{L}\right], \tag{3}$$

results in a natural frequency of

$$\omega^2 = \frac{1}{3m}\left[EI\left(\frac{2\pi}{L}\right)^4 - P\left(\frac{2\pi}{L}\right)^2\right]. \tag{4}$$

From this we immediately see that buckling occurs when $P_{cr} = EI(2\pi/L)^2$ (exact) and in the absence of the axial load we obtain a natural frequency of $\omega_0 = 22.79\sqrt{EI/(mL^4)}$ (exact coefficient $= 22.37$). Using these to nondimensionalize ($\bar{p} = P/P_{cr}$ and $\bar{\omega} = \omega/\omega_0$ we have

$$\bar{\omega}^2 = 1 - \bar{p}. \tag{5}$$

Now, subjecting the system to a transverse harmonic point force at mid-span, $F(t)$, and assuming a small amount of linear viscous damping, C, we have the equation of motion given by equation (1) in which

$$x = Q, \quad M = 3m, \quad K = EI(2\pi/L)^4, \quad p = P/P_{cr} \tag{6}$$

and the corresponding receptance is still given by equation (2).
A closely related circumstance is what happens when the support upon which the mass is supported is excited, e.g., $z(t) = z_0 \sin \omega t$, i.e., transmissibility.

The response can also be plotted as a contour plot in terms of axial load and forcing frequency. This is shown below. In this plot we can observe how the resonant peaks spread as the axial load is increased. This can be viewed as an increase in the damping ratio (since this is relative to the natural frequency and hence stiffness).

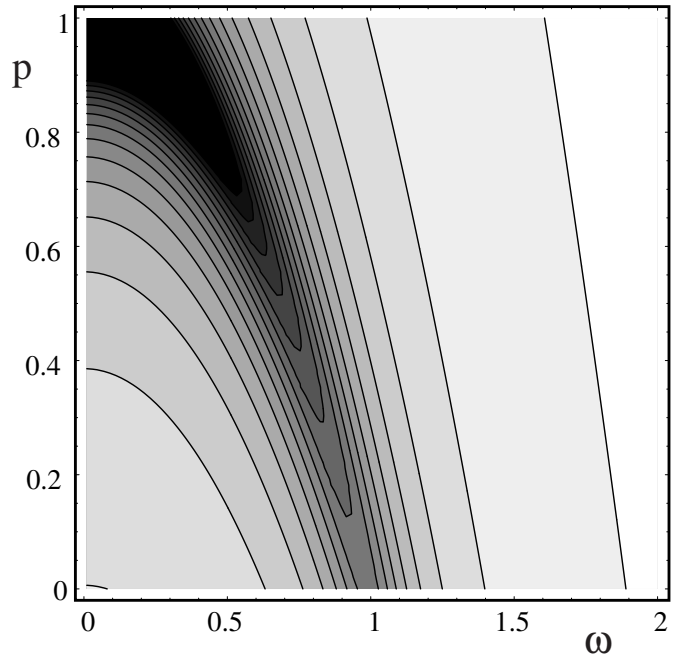

Effect of axial load on the receptance of a damped, SDOF model of a beam as a contour plot. Darker shade are higher in magnitude. $C = 0.1$.

We can again obtain a useful physical sense of the effect of the changing axial load on the forced vibration problem by evolving the axial load as a linear function of time: $p = 0.002t$. In this way, the stiffness of the system will reduce to zero when $t = 500$. The figure below shows an example based on numerical simulation of the governing equation of motion including the diminishing stiffness. The forcing parameters are fixed at $F_0 = 1, \omega = 0.5$ and hence resonance should occur when $t \approx 375$.

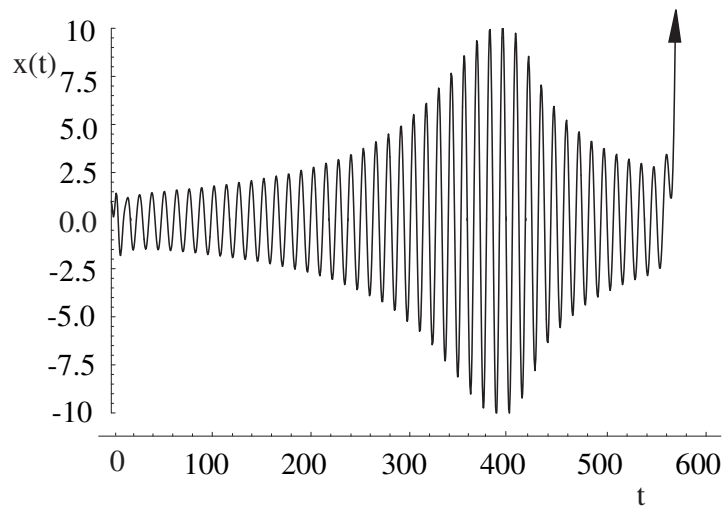

A sweep through decaying stiffness and passing through resonance.

Note that there is again a small amount of overshoot in the non-stationary (slowly evolving, or swept) response.

Beyond Buckling

We can extend the single-mode energy analysis of this system by including higher order terms in the potential energy of this system (truncated after the second term)

$$V = \frac{1}{2}EI\int_0^L \left[w''^2 + w''^2 w'^2\right] dx - \frac{1}{2}P\int_0^L \left[w'^2 + \frac{1}{4}w'^4\right] dx, \qquad (7)$$

and the kinetic energy remains the same. Evaluating the potential energy expression now gives

$$\begin{aligned} V &= \frac{1}{16}EIL\left(\frac{2\pi}{L}\right)^4 Q^2 + \frac{1}{256}EIL\left(\frac{2\pi}{L}\right)^6 Q^4 \\ &\quad -\frac{1}{16}PL\left(\frac{2\pi}{L}\right)^2 Q^2 - \frac{1}{128}P\frac{3L}{8}\left(\frac{2\pi}{L}\right)^4 Q^4. \end{aligned} \qquad (8)$$

In addition to the trivial ($Q = 0$) solution we now have a non-trivial (post-buckled) path given by

$$Q^2 = \frac{8(\bar{p} - 1)}{(\frac{2\pi}{L})^2(1 - \frac{3}{4}\bar{p})}, \tag{9}$$

where

$$\bar{p} = \frac{P}{EI(\frac{2\pi}{L})^2}. \tag{10}$$

Also, after buckling, the nondimensional natural frequency is given by

$$\bar{\omega}^2 = 1 + \frac{3(\bar{p} - 1)}{(1 - \frac{3}{4}\bar{p})} - \bar{p}\left[1 + \frac{\frac{9}{4}(\bar{p} - 1)}{(1 - \frac{3}{4}\bar{p})}\right] = \bar{\omega}^2 = 2(\bar{p} - 1), \tag{11}$$

i.e., half the pre-buckling slope of the load-frequency (squared) relation (equation 5). This is a result anticipated from the normal form of the supercritical pitchfork bifurcation.

The Poincaré Section

Before moving on to consider the resonance response of axially-loaded continuous systems we introduce the concept of Poincaré sampling. The response of the forced nonlinear oscillator of the type of equation (1) with $p = 0$ is typically given in terms of transient and steady-state parts. In the framework of dynamical system theory we can view the steady state as a periodic attractor for the surrounding transients. For a linear system the periodic attractor is unique. This is not necessarily the case for nonlinear oscillators. A typical engineering approach is then to plot the maximum amplitude of response as a function of the forcing frequency. Often the phase difference between the forcing function and the response is also plotted and a sudden shift in phase is associated with resonance. However, an alternative description of the response is to reduce the 3D phase space in continuous time to a 2D phase space in discrete time, via Poincaré sampling.

The complete solution to equation (1) with $p = 0$ can be written as

$$x(t) = \frac{F_0}{K} \frac{\sin(\omega t - \phi)}{\sqrt{\left[1 - (\omega/\omega_n)^2\right]^2 + \left[2\zeta\omega/\omega_n\right]^2}} + X_1 e^{-\zeta\omega_n t} \sin(\sqrt{1-\zeta^2}\omega_n t + \phi_1), \tag{12}$$

and focusing on the steady-state solution we ignore the second term and write equation (12) in the alternative form

$$x(t) = a\cos(\omega t) + b\sin(\omega t). \tag{13}$$

Differentiating this to get the velocity, we have

$$y(t) \equiv \dot{x} = -a\omega \sin(\omega t) + b\omega \cos(\omega t), \tag{14}$$

and setting $t = 0$ (which effectively fixes the initial forcing phase) we simply get $x = a$ and $y = b\omega$ as the fixed point location, where

$$a = \frac{(1 - \Omega^2)f}{(1 - \Omega^2)^2 + (2\zeta\Omega)^2} \tag{15}$$

and

$$b = \frac{2\zeta\Omega f}{(1 - \Omega^2)^2 + (2\zeta\Omega)^2}, \tag{16}$$

and $\Omega = \omega/\omega_n$. The Poincaré section can thus be considered as an alternative to the more conventional (amplitude-phase) representation of the response of an oscillator.

The complementary function (the transient solution) can also be included in the following way to give a discrete mapping: the Poincaré map P,

$$\begin{pmatrix} x \\ y \end{pmatrix} \rightarrow e^{\frac{-2\pi\zeta\omega_n}{\omega}} \begin{bmatrix} C + \frac{\zeta\omega_n}{\omega_d}S & \frac{1}{\omega_d}S \\ -\frac{\omega_n^2}{\omega_d}S & C - \frac{\zeta\omega_n}{\omega_d}S \end{bmatrix} \begin{pmatrix} x \\ y \end{pmatrix} + e^{\frac{-2\pi\zeta\omega_n}{\omega}} \begin{pmatrix} -aC + (-\frac{\zeta\omega_n a}{\omega_d} - \frac{b\omega}{\omega_d})S \\ -b\omega C + (\frac{a\omega_n^2}{\omega_d} + \frac{\zeta b\omega_n\omega}{\omega_d})S \end{pmatrix} + \begin{pmatrix} a \\ b\omega \end{pmatrix} \quad (17)$$

where $C \equiv \cos(2\pi\omega_d/\omega)$ and $S \equiv \sin(2\pi\omega_d/\omega)$, and $\omega_d = \omega_n\sqrt{1-\zeta^2}$.

Thus, given some initial conditions, this set of difference equations will map out the transient at intervals of the forcing period until converging on the fixed point

$$(x, y) = (a, b\omega). \tag{18}$$

This mapping is exact for a linear oscillator (and is related to the Z-transform) but cannot usually be easily obtained for nonlinear systems. However, importantly, this complete mapping contains the stability information regarding the fixed point, and relates back to Floquet theory and characteristic multipliers.

We have already introduced the concept of characteristic eigenvalues (CEs) determining stability of equilibria in unforced systems. Now we see that it is the eigenvalues of the map (characteristic multipliers - CMs) that determine the stability of cycles. The eigenvalues of the Jacobian, i.e., the first partial derivatives of the map given by equation (17), $DP(a, \omega b)$, are given by

$$\lambda_{1,2} = e^{-\frac{2\pi\zeta\omega_n}{\omega} \pm i\frac{2\pi\omega_d}{\omega}}, \tag{19}$$

which confirms that the fixed point is asymptotically stable, since the damping and natural frequency are positive numbers. This is why consideration of discrete maps plays a useful role in the study of flows.

Continuous Systems

We now turn to consideration of axially-loaded, transversely forced, continuous beams. A beam of length L, mass per unit length m, uniform flexural rigidity EI, viscous damping coefficient C, axial force P, and transverse load $Q_0 F(x) \cos \Omega t$, responds as $w(x, t)$. The governing equation of motion is

$$m w_{tt} + C w_t + EI w_{xxxx} + P w_{xx} = Q_0 F(x) \cos \Omega T \tag{20}$$

in which subscripts on w reflect partial derivatives.

The governing equation can be put in the nondimensional form

$$\frac{\partial^4 \bar{w}}{\partial \bar{x}^4} + c\frac{\partial \bar{w}}{\partial \bar{t}} + p\frac{\partial^2 \bar{w}}{\partial \bar{x}^2} + \frac{\partial^2 \bar{w}}{\partial \bar{t}^2} = f(x)\cos\bar{\Omega}\bar{t}, \tag{21}$$

using

$$\begin{aligned} \bar{x} &= x/L, & \bar{w} &= w/L, & \bar{t} &= t\sqrt{EI/(mL^4)}, \\ p &= PL^2/(EI), & \bar{\Omega} &= \Omega\sqrt{mL^4/(EI)}, & c &= CL^2/\sqrt{mEI}, \\ f(x) &= Q_0 F(X)L^3/(EI), & \zeta &= c/(2\Omega_1), \end{aligned} \tag{22}$$

where Ω_1 is the fundamental natural frequency and its value depends on the boundary conditions.

For convenience, we now drop the overbar notation, and assuming a steady-state harmonic response of the form

$$w(x,t) = Re\left[y(x)e^{i\Omega t}\right], \tag{23}$$

leads to

$$y''''(x) + py''(x) + (i\Omega c - \Omega^2)y(x) = f(x). \tag{24}$$

This equation can then be solved for a specific set of boundary conditions and transverse forcing types. Here, two cases will be considered:

- An axially-loaded cantilever beam with a uniformly distributed harmonic load,
- An axially-loaded, clamped-clamped beam with a harmonic central point load.

Considering the first case as shown below

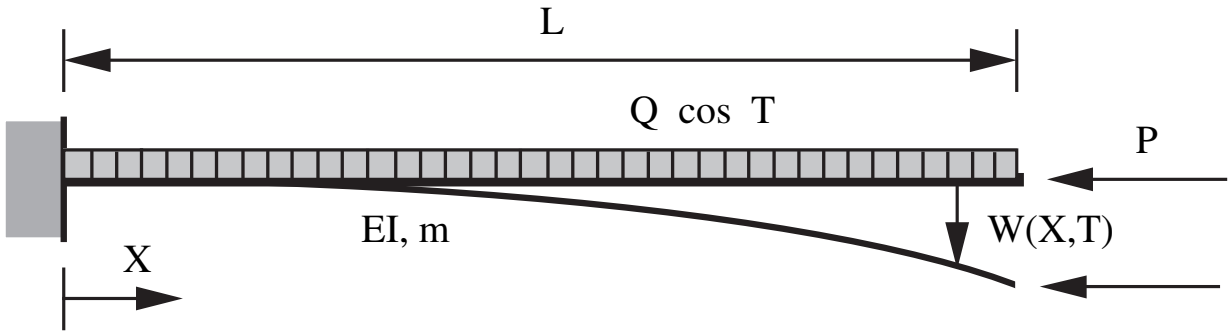

A cantilever beam subject to a constant axial load and a harmonically-varying uniformly distributed lateral force.

we have a governing equation of motion given by equation (24) but now with unity on the right hand side.

The general solution is given by

$$y(x) = (i\Omega c - \Omega^2)^{-1} \sum_{j=1}^{2} (a_j \cosh \lambda_j x + b_j \sinh \lambda_j x), \tag{25}$$

where

$$\lambda_j = (\nu_j/\gamma_j) + i(\gamma_j/2), \qquad \gamma_j = \left[2\left[-\epsilon_j + \sqrt{\epsilon_j^2 + \nu_j^2}\right]\right]^{1/2}$$

$$\nu_1 = \phi/2, \qquad \nu_2 = -\phi/2,$$

$$\epsilon_1 = (\Phi - p)/2, \qquad \epsilon_2 = -(\Phi + p)/2$$

$$\Phi = -\frac{c\Omega}{2\phi}, \quad \phi = \left[\left[-\delta + \sqrt{\delta^2 + (c\Omega)^2}\right]/2\right]^{1/2}$$

$$\delta = p^2 + 4\Omega^2.$$

The boundary conditions in this case are $y(0) = 0, y'(0) = 0, y''(1) = 0$, and $y'''(1) + py'(1) = 0$. The elastic critical load is $p_{cr} = \pi^2/4$, and the fundamental natural frequency is $\Omega_1 = 3.516$. Applying the boundary conditions and solving the resulting simultaneous equations (in a_j, b_j) leads to the results shown in the next slide in which a damping ratio of $\zeta = 0.142$ was used.

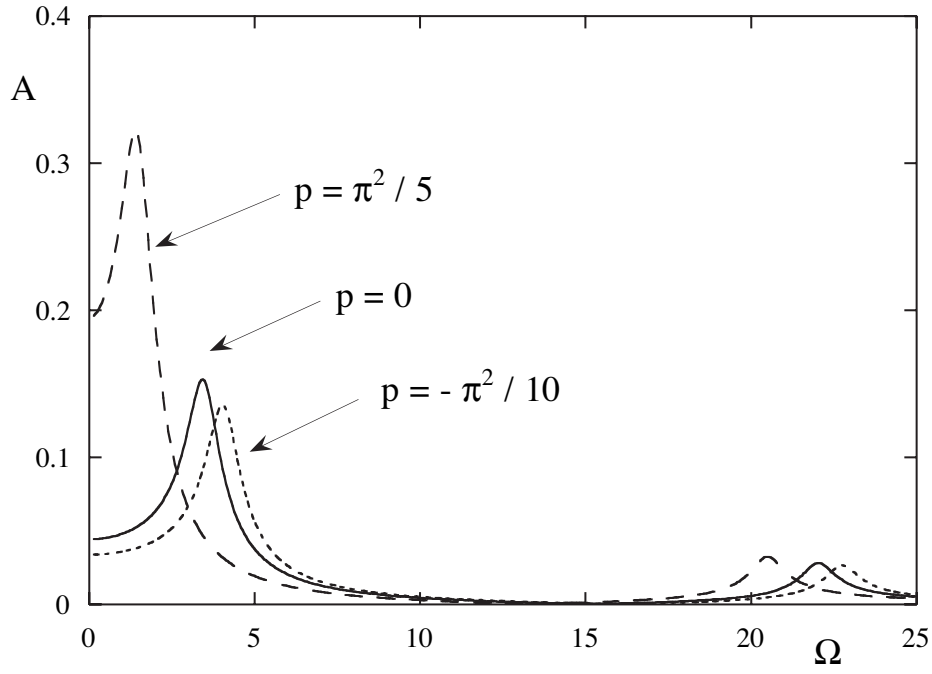

The central amplitude versus the forcing frequency for a cantilever beam with a uniformly distributed force.

The amplitude A is the magnitude of the maximum central deflection, which depends on the static axial load and the forcing frequency, i.e., $A(\Omega, p) = |y(0.5)|$. Note the presence of the second resonant peak in the vicinity of $\Omega = 22$.

It is interesting to see how the amplitude (and the corresponding resonant frequency) vary with axial load. The figure below shows the relation

$$A_R(p) = \max_{\Omega \geq 0} A(\Omega, p), \tag{26}$$

and the values of Ω (squared) for which this condition occurs (using three representative damping values).

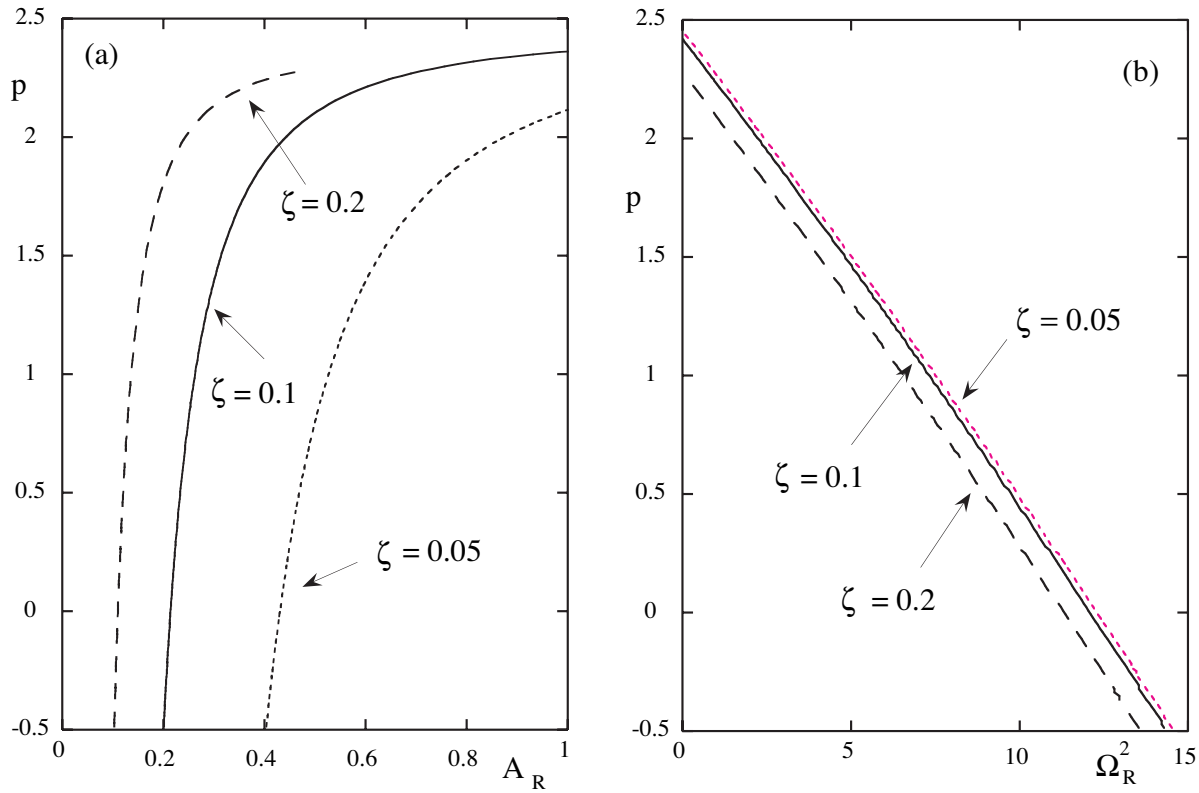

(a) The resonant amplitude, (b) the frequency squared versus the axial load for a cantilever beam with a uniformly distributed force.

Now consider the second case. In part (a) of the figure shown below the amplitude response (receptance) when $\zeta = 0.02$. We again see the anticipated increase in natural frequency for a tensile axial force, and reduction for compression.

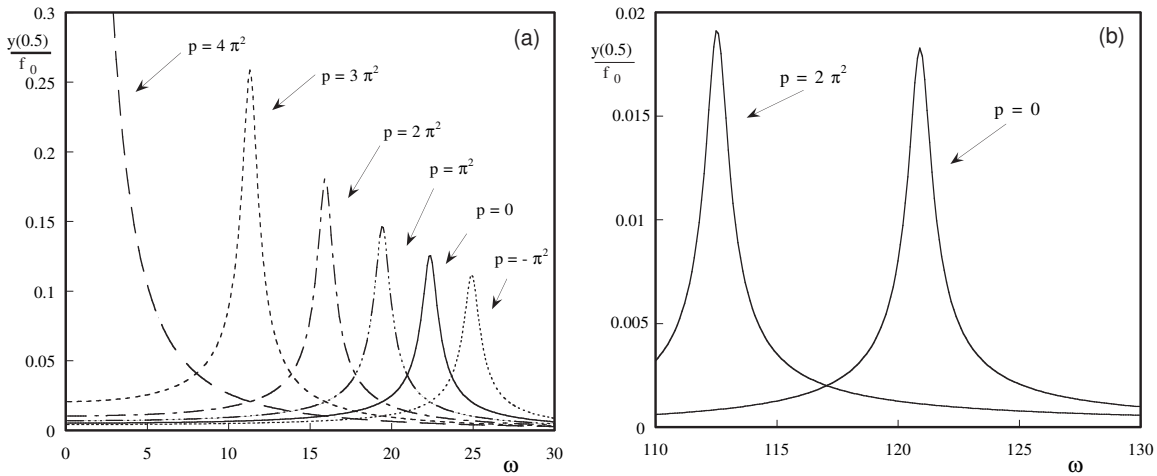

(a) Amplitude response of an axially-loaded, clamped-clamped beam subject to a central point harmonic point force, (b) in the vicinity of the third mode.

Part (b) of the preceding figure shows how the receptance associated with the third (second symmetric) mode is affected by the presence of an axial load. In this case the undamped third frequency occurs at $\Omega = 120.9$ for the unloaded case. The peaks are also shifted slightly from those of the undamped case due to the presence of a little damping.
In both of the examples above, it can be shown that the resonant amplitude and frequency are given approximately by

$$A_R(p) \approx A_R(0)/\sqrt{1-(p/p_{cr})} \quad (27)$$

$$\Omega_R^2 \approx \Omega_1^2[1-(p/p_{cr})], \quad (28)$$

and we can also relate this back to the (unforced) material presented earlier, e.g., the $p = 0$ resonant peak for the beam occurs at the natural frequency coefficient of 22.4.

Experimental Verification

A thin steel strip was clamped between blocks at its ends and placed in a displacement-controlled testing machine. In this configuration the end shortening is prescribed and the resulting axial force is measured using a load cell. With the standard expressions based on the earlier analysis, the critical load was computed at 1,235N and the lowest natural frequency (with no axial load) at 44Hz. The strut was struck by an impact hammer and a laser velocity vibrometer was used to measure the response. The data were then acquired and analyzed using the Bruel Kjaer (B&K) PULSE system. Velocity time series were then subject to a Hanning window and an FFT algorithm to extract the frequency content. This process was repeated 10 times at each axial load level. The results were averaged and displayed as normalized mobility, i.e., normalized with respect to the force of the impact hammer.

A photograph of the experimental system is shown below in (a).

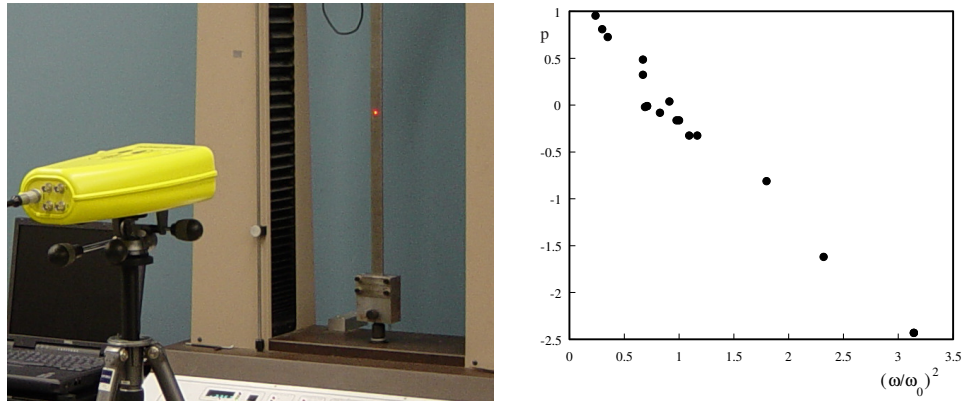

(a) A photograph of the clamped beam in the testing machine, (b) the axial load plotted as a function of the natural frequencies (squared).

Part (b) shows a summary of how the peaks shift to lower (higher) frequency as the compressive (tensile) axial load is increased. However, experimental results from this type of system need careful consideration because testing machines are sometimes referred to as semi-rigid loading devices, membrane effects in the beam may occur, and even the boundary conditions can be a function of loading.

Topics *not* covered

- Discrete models
  - asymmetric discrete models
  - 2 dof Augusti model
  - multiple loads
  - Load dependent supports
  - Path-following (continuation)
- Strings, cables and membranes
- Continuous beams
  - Tangential loading
  - Modal coupling
  - Flexural-torsional effects
  - Shallow arches
- Plates
  - Large deflections
  - Circular plates
  - Mode jumping
  - Cylinders
- Highly-deformed structures
- Suddenly applied loads
- Pulsating axial loads
- Nonlinear vibration